Paper:

Fault-Tolerant Control for Manipulator under Actuator Fault with Output Constraint

Yong Hu, Fengjuan Xu, Yun Li,Yaobing Li*, Jianlei Gao, Tianyu Gong

Institute of Baozhang China Industrial Control Systems Cyber Emergency Response Team, Beijing 100040, P. R. China
E-mail:32201906862@bit.edu.cn,liyaobing@cics-cert.org.cn

[Received 00/00/00; accepted 00/00/00]

This paper investigates motion control problems of robotic manipulators under the actuator fault. The uncertainty induced by actuator faults brings up great challenges to control method design. Besides, with the consideration of output constraint and disturbance simultaneously, a fault-tolerant control (FTC) scheme, oriented to solve motion control problems is proposed in this paper. The barrier Lyapunov function is employed to deal with output constraint, an extended state observer (ESO) is used to compensate the system perturbation such as parameter uncertainties and external disturbance, and a fault estimation observer (FEO) is designed to compensate the actuator fault. Theoretical results are shown to confirm the output constraints are not violated and all the desired signals in the system are uniformly bounded. The simulation results verify the effectiveness and robustness of the proposed control scheme.

Keywords: fault-tolerant control (FTC), barrier Lyapunov function, output constraint, robotic manipulator

1. INTRODUCTION

With the rapid development of computer technology and the growing demand for automation, the robotic manipulator control has emerged as an important area of research. According to the Global Robotic Arm Market report [2], The compound annual growth rate of the global robotic manipulator market will exceed 13.8%, from 17.9 billion in 2018 to 39.2 billion in 2024. Stability and reliability are crucial factors for the robotic manipulator to be widely implemented [14].

As a multi-input multi-output (MIMO) nonlinear system, the manipulator has uncertainties such as parameter perturbation, external disturbance and unmodeled dynamics et al.[11]. Apart from the uncertainty, system faults may also exist in controllers, actuators, plants, sensors, etc. The actuator, as the primary component of the system, might be significantly affected by these faults. Especially in hard environmental conditions, such as particle radiation, electromagnetic interference, etc. Faults may occur more easily. Therefore, the performance of the robotic arm will be greatly degraded, and even the mission will fail in severe cases. However, manual repair in outer space is almost impossible. Manipulators need to tolerate failures and continue to perform given operational tasks reliably. Consequently, fault-tolerant control (FTC) [15] is essential for the safety of the robotic manipulator.

At present, to tackle the fault of the system, there exist quantities of FTC schemes such as adaptive FTC [4], sliding mode FTC [5], and neural network FTC [8]. Hamid et al. defined the optimality as the minimum end-effector velocity jump, then they designed an optimal redistribution control scheme of joint velocities and verified the effectiveness of this method through simulation[1]. In terms of passive fault-tolerant control, Van et al. proposed a new robust robot controller by designing a sliding mode surface based on PID-non-singular fast terminal sliding mode control, which realized many advantages such as fast transient response, chattering elimination and finite time convergence[13].

Compared with the above-mentioned FTC schemes, the active-FTC method has the attractive advantages of simple design and unified control structure due to its ability to obtain fault information. Considering that the fault observation based on the neural network requires the powerful computing power of a robot manipulator, which means it is difficult to be implemented in practical applications. Considering the above problems, some literature tends to avoid using neural networks. Zhang et al. proposed an equivalent system of fixed-time sliding mode control. This method eliminates the influence of actuator validity failure through system transformation, and at the same time can deal with the constraints of system uncertainty[16].

At the same time, how to ensure the motion constraints under the actuator fault is also a problem to be solved. The barrier Lyapunov function (BLF) is widely used in output constrained control. The basic idea of BLF is that when the value of the output variable tends to set the boundary, the value of BLF tends to infinity. In [6], Chen et al. proposed a non-singular fast terminal sliding mode control method based on the BLF of the non-recursive disturbance observer. By designing BLF to constrain the sliding mode variable, the sliding mode variable can satisfy the output tracking error constraint.

. Corresponding author:Yaobing Li, liyaobing@cics-cert.org.cn.
Supported by National Key R&D Program of China under Grant 2021YFB2012404.

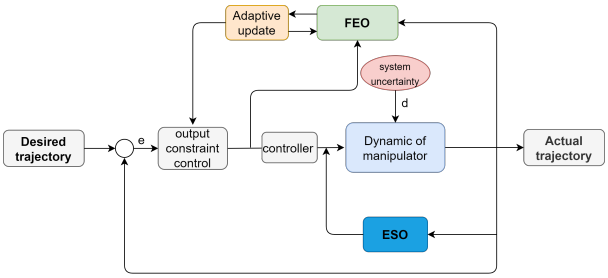


Fig. 1. Structure of the proposed controller.

In this paper, the external disturbance, actuator faults and output constraints are considered simultaneously, and we proposed a composite fault-tolerant control scheme which shows as Fig 1. The active fault-tolerant control scheme designed for the faults uses a fault estimation observer, which detects the fault more accurately and estimates it in real-time. The main contributions of this article are as follows.

1. A composite control scheme is proposed for actuator failures. Furthermore, a adaptive update law for fault estimation observer is designed which achieved robust observation performance of faults.

2. When designing the controller, the barrier Lyapunov function is introduced for the output constraint. And the system output error remains within the set range effectively.

2. ROBOT DYNAMICS DESCRIPTION AND PROBLEM STATEMENT

2.1. Dynamic of Manipulator

Considering a n-joint robot manipulator with actuator failure, the dynamics of the system can be expressed as

$$M(q)\ddot{q}+C(q,\dot{q})\dot{q}+G(q)+\tau_d = D(\tau) \quad . \quad . \quad . \quad (1)$$

where $q,\dot{q},\ddot{q} \in R^n$ are the vector of joint generalized position, velocity, and acceleration, respectively. $M(q) \in R^{n\times n}$ denotes inertia matrix. $C(q,\dot{q}) \in R^{n\times n}$ is the Coriolis and centrifugal matrix. $G(q) \in R^n$ is the gravitational force. $D(\tau)$ is the actuator failure function which $\tau \in R^n$ is the vector of joint torques supplied by the actuators and τ_d represents external disturbances to the manipulator.

Property 1: [10] The matrix $\dot{M}(q)-2C(q,\dot{q})$ is a skew symmetric matrix.

Property 2: [9] The inertia matrix $M(q)$ satisfies the following inequality

$$m_1\|x\|^2 \le x^T M(q)x \le m_2\|x\|^2 \quad . \quad . \quad . \quad . \quad . \quad . \quad . \quad (2)$$

where m_1, m_2 are positive constants.

2.2. Actuator Faults

As discussed in [3], the actuators are sensitive to two main faults: (1) constant gain fault; (2) constant deviation fault. Both (1) and (2) can be mathematically modeled as follows.

2.2.1. Constant Gain Fault

When the constant gain fault occurs, the fault model equation is as following

$$D(\tau) = \rho\tau, \rho = \mathrm{diag}\{\rho_i\} \quad , \quad i = 1,2,\ldots,n \quad . \quad (3)$$

This type of fault means that the actuator has loss of effect (LOE) fault, which causes the actual output control torque to be proportional to the expected value. ρ_i represents the effective factor of the actuator, that is, the degree of failure. When $\rho_i = 1$, it means that the actuators are working normally and no failure occurs; when $\rho_i = 0$, it means that the actuator is completely invalid; when $\rho_i \in (0,1)$, it means that the system has an actuator constant gain (multiplier) failure, that is, a partial failure here.

2.2.2. Constant Deviation Fault

When the constant deviation fault occurs, the fault model equation is as following.

$$D(\tau) = \tau + f_u, f_u = [f_{u1}, f_{u2}, \cdots, f_{un}]^T \quad . \quad . \quad . \quad . \quad (4)$$

This type of fault means that one or more inputs have been added to the system, resulting in a fixed deviation of the actual output control torque from the expected value. Among them, τ represents the expected value of the control torque, $D(\tau)$ represents the actual value of the control torque, and f_u is the fault item. When $f_u = 0$, it means that the system works normally.

The control outputs in the equations (3) and (4) are based on the different fault types when the values of the applied disturbance torque f_u and the actuator fault factor ρ change.

In the actual situation, the two kinds of faults may occur at the same time, so considering the various faults of the robot manipulator comprehensively.

The fault can be represented as

$$D(\tau) = \rho\tau + f_u \quad . \quad . \quad . \quad . \quad . \quad . \quad . \quad . \quad . \quad . \quad . \quad . \quad (5)$$

The control objective is to enable the robotic manipulator to track the desired trajectory effectively in the event of a robot system failure. The following are the assumptions commonly found in related research

Assumption 1: [17] The system uncertainty and the constant deviation fault d is a bounded uncertain constant.

Assumption 2: (Bounded Desired Trajectory) The desired trajectory is known, continuous and bounded, It means $||q_d| \le Q_d$ with Q_d a known bound.

3. DESIGN COMPOSITE CONTROL

3.1. Fault Estimate Observer

In the fault model equation (3) of constant gain fault, the failure factor $\rho \in R^{n\times n}$ is a diagonal matrix. In order

to facilitate to estimate the fault factor, the term $\rho\tau$ in equation (3) can be rewritten as follow

$$\rho\tau = Uv \quad . \quad . \quad . \quad . \quad . \quad . \quad . \quad . \quad . \quad . \quad . \quad . \quad . \quad . \quad . \quad (6)$$

where $U = diag[\tau_1, \tau_2, \cdots, \tau_n], v = [\rho_1, \rho_2, \cdots, \rho_n]^T$.

Then the dynamic equation (1) of the manipulator under actuator failure can be rewritten as follows

$$M(q)\ddot{q} + C(q,\dot{q})\dot{q} + G(q) = Uv + d \quad . \quad . \quad . \quad . \quad . \quad (7)$$

where d denotes the system uncertainty and the constant deviation fault, which is represented as

$$d = -\tau_d + f_u \quad . \quad . \quad . \quad . \quad . \quad . \quad . \quad . \quad . \quad . \quad . \quad . \quad . \quad . \quad . \quad (8)$$

In order to estimate the disturbance in the system accurately, we apply the ESO to observe the disturbance of the system.

Generally speaking, it is difficult to measure the external disturbance without definite mathematical model directly, but we can estimate the internal state variables and external total disturbance accurately in real time by using ESO.

To facilitate ESO design, in view of (7), we can derive that

$$\ddot{q} = M(q)^{-1}[-C(q,\dot{q}) - G(q) + d] + M(q)^{-1}Uv \quad (9)$$

Assuming $f_1(t) = M(q)^{-1}[-C(q,\dot{q}) - G(q)]$ and $f_2(t) = M(q)^{-1}d$, then we get

$$\ddot{q} = f_1(t) + f_2(t) + M(q)^{-1}Uv \quad . \quad . \quad . \quad . \quad . \quad . \quad . \quad . \quad (10)$$

By denoting the vectors $q_1 = q$, $q_2 = \dot{q}$,$\dot{q}_3 = f_2(t)$ the dynamics (10) can be expressed as the extended order system

$$\begin{cases} \dot{q}_1 = q_2 \\ \dot{q}_2 = f_1(t) + q_3 + M(q)^{-1}Uv \\ \dot{q}_3 = f_2(t) \\ y = q_1 \end{cases} \quad . \quad . \quad . \quad . \quad . \quad . \quad (11)$$

An ESO is designed as follows

$$\begin{cases} \dot{z}_1 = z_2 - \beta_{01} g_1(z_1 - q_1) \\ \dot{z}_2 = f_1(t) + z_3 - \beta_{02} g_2(z_1 - q_1) + M^{-1}Uv \\ \dot{z}_3 = -\beta_{03} g_3(z_1 - q_1) \end{cases} \quad (12)$$

The form of nonlinear function $g_i(e)(i = 1, 2, \cdots, n+1)$ [7] is as follows

$$g_i(e) = fal(e, \alpha_i, \delta) = \begin{cases} |e|^{\alpha_i} \operatorname{sgn} e, |e| > \delta \\ e/\delta^{1-\alpha_i}, |e| \le \delta \end{cases} \quad . \quad (13)$$

where $0 < \alpha_i < 1$ and $\delta > 0$, and z_3 is an expanded variable.

According to z_3, the total disturbance $f_2(t)$ of the manipulator system can be estimated in real time. Then, for the case of actuator failure in the manipulator system, in order to estimate and compensate actuator failure ρ, a fault estimation observer (FEO) is designed

$$\begin{cases} \dot{\hat{q}}_2 = -L(\hat{q}_2 - q_2) + M^{-1}\left(-Cq_2 - G + \hat{d} + U\hat{v}\right) \\ \dot{\hat{v}} = U^T M^{-1}\tilde{q}_2 \end{cases} \quad (14)$$

where $\hat{q}_2 \in R^n$ denotes the estimated value of q_2, L is the adaptive gain, and $\hat{v} = [\hat{\rho}_1, \hat{\rho}_2, \cdots \hat{\rho}_n]^T$. Estimation error is $\tilde{q}_2 = q_2 - \hat{q}_2$.

In view of (10) and (14), we can derive that the fault estimation observer error dynamic equation as

$$\dot{\tilde{q}}_2 = -L\tilde{q}_2 + M^{-1}\tilde{d} + M^{-1}U\tilde{v} \quad . \quad . \quad . \quad . \quad . \quad . \quad . \quad (15)$$

where $\dot{\tilde{q}}_2 \in R^n$, and $\tilde{d} = d - \hat{d}$, which is observed by ESO.

Based on the above analysis, the main conclusions can be obtained

theorem 1: for the manipulator system (7) with actuator multiplicative failure, a fault estimation observer (14) is designed, and the online real-time estimation of the failure is realized. The design of the adaptive law $\dot{\hat{v}} = U^T M^{-1}\tilde{q}_2$ can ensure that the asymptotic stability of the observer.

Proof: The proof procedures are presented as follows.

Choose following Lyapunov function

$$V = \frac{1}{2}\tilde{q}_2^T\tilde{q}_2 + \frac{1}{2}\tilde{v}^T\tilde{v} \quad . \quad . \quad . \quad . \quad . \quad . \quad . \quad . \quad . \quad . \quad . \quad . \quad (16)$$

Computing the time-derivative of V, we can derive that

$$\begin{aligned} \dot{V} &= \tilde{q}_2^T\dot{\tilde{q}}_2 - \tilde{v}^T\dot{\hat{v}} \\ &= -\tilde{q}_2^T L\tilde{q}_2 + \tilde{q}_2^T M^{-1}\tilde{d} + \tilde{q}_2^T M^{-1}U\tilde{v} - \tilde{v}^T\dot{\hat{v}} \end{aligned} \quad . \quad (17)$$

Bring the adaptive law into the equation (17). When $t \to \infty$, then $\hat{d} \to d$. Therefore,

$$\dot{V} = -\tilde{q}_2^T L\tilde{q}_2 \le 0 \quad . \quad . \quad . \quad . \quad . \quad . \quad . \quad . \quad . \quad . \quad . \quad . \quad (18)$$

Choosing the appropriate size of the matrix L, we can derive that $\tilde{q}_2^T L\tilde{q}_2 \ge 0$. Then the equation (18) can be easily established. Thus, the designed observer can guarantee global asymptotic stability. The proof is completed. ■

3.2. Output Constraint

In order to facilitate the design of the controller, the following lemma is given.

lemma 1: [12] For any positive constant vector $b \in R^n$ and any vector $z \in R^n$ which $|z| < |b|$, the following inequality always hold

$$\ln \frac{b^T b}{b^T b - z^T z} \le \frac{z^T z}{b^T b - z^T z} \quad . \quad . \quad . \quad . \quad . \quad . \quad . \quad . \quad . \quad (19)$$

From (9), we can rewrite the dynamics of the robotic manipulator as

$$\begin{cases} \dot{q}_1 = q_2 \\ \dot{q}_2 = M^{-1}(-Cq_2 - G + d) + M^{-1}\rho\tau \\ y = q_1 \end{cases} \quad . \quad . \quad (20)$$

First we let

$$\begin{cases} e_1 = q_1 - q_d \\ e_2 = q_2 - \beta \end{cases} \quad . \quad . \quad . \quad . \quad . \quad . \quad . \quad . \quad . \quad . \quad . \quad . \quad (21)$$

where $q_d \in R^n$ denotes the desired trajectory, and β is the stabilizing control function. Then $\dot{e}_1 = \dot{q}_1 - \dot{q}_d$, which e_1 denotes the trajectory tracking error.

Design the virtual control β as

$$\beta = -K_1 e_1 + \dot{q}_d \quad . \quad . \quad . \quad . \quad . \quad . \quad . \quad . \quad . \quad . \quad . \quad . \quad . \quad (22)$$

where $K_1 = diag[k_1, k_2, \cdots, k_n]$, and $k_i \geq 0$.

In view of (21) and (22), we can derive that

$$\dot{e}_1 = -K_1 e_1 + e_2 \quad . . . . . (23)$$

We choose the following barrier Lyapunov function as

$$V_1 = \frac{1}{2}\sum_{i=1}^{n} \ln \frac{b_i^2}{b_i^2 - e_{1i}^2} \quad . . . . . (24)$$

The derivative of V_1 is given as

$$\dot{V}_1 = \sum_{i=1}^{n} \frac{-k_i e_{1i}^2 + e_{1i} e_{2i}}{b_i^2 - e_{1i}^2} \quad . . . . . (25)$$

Then design the model-based control as

$$\tau = \hat{\rho}^{-1}(-K_2 e_2 - \xi + C\beta + G + M\dot{\beta} - d) \quad . . (26)$$

where $K_2 = K_2{}^T \geq 0_{n\times n}$, $\xi = \begin{bmatrix} \frac{e_{11}}{b_1^2 - e_{11}^2} \\ \frac{e_{12}}{b_2^2 - e_{12}^2} \\ \vdots \\ \frac{e_{1n}}{b_n^2 - e_{1n}^2} \end{bmatrix}$.

Lyapunov function V_2 is defined as

$$V_2 = V_1 + \frac{1}{2} e_2^T M(q_1) e_2 \quad . . . . . (27)$$

The time-derivative of V_2 can be obtained as

$$\dot{V}_2 = \dot{V}_1 + e_2^T M(q_1)\dot{e}_2 + e_2^T \frac{1}{2}\dot{M}(q_1) e_2 \quad . . . (28)$$

Substituting (20) and (21) into (28) results in

$$\dot{V}_2 = \dot{V}_1 + e_2^T \left[\rho\tau + \hat{d} - C(q,\dot{q})\beta - G(q) - M(q)\dot{\beta}\right] (29)$$

Applying the composite control laws (26), when $t \to \infty$, $\hat{d} \to d$. Equation (29) can be transformed into

$$\dot{V}_2 = \dot{V}_1 + e_2^T[(\hat{\rho} + \tilde{\rho})\hat{\rho}^{-1}(-K_2 e_2 + \varpi + \xi) - \varpi] (30)$$

where $\varpi = C\beta + G + M\dot{\beta} - d$, and $\tilde{\rho} = \rho - \hat{\rho}$.

So we can get

$$\dot{V}_2 = -\sum_{i=1}^{n} \frac{k_i e_{1i}^2}{b_i^2 - e_{1i}^2} - e_2^T K_2 e_2 - e_2^T \varepsilon \quad . . . . . (31)$$

where

$$\varepsilon = \tilde{\rho}\hat{\rho}^{-1}(K_2 e_2 + \xi - \varpi) \quad . . . . . (32)$$

Also $-e_2^T\varepsilon \leq e_2^T e_2 + \frac{1}{2}||\varepsilon||^2$ implies

$$\dot{V}_2 \leq -\sum_{i=1}^{n} \frac{k_i e_{1i}^2}{b_i^2 - e_{1i}^2} - e_2^T(K_2 - I)e_2 + \frac{1}{2}||\varepsilon||^2 \quad . (33)$$

According to the Lemma 1, if the parameters K_1, K_2 have been chosen properly, there exist positive numbers α and λ to guarantee the following formula holds true

$$\dot{V}_2 \leq -\alpha V_2 + \lambda \quad . . . . . (34)$$

where

$$\alpha = \min\left\{2\min(k_i), \frac{2\lambda_{\min}(K_2 - I)}{\lambda_{\max}(M)}\right\} \quad . . . (35)$$

$$\lambda = \frac{1}{2}||\varepsilon||^2 \quad . . . . . (36)$$

Combining the above design process, the following theorem is obtained.

theorem 2: Consider the robot manipulator system (1), which includes unknown disturbance, actuator failures and output constraints. The proposed composite control ensures that

1. The closed loop signals e_1, e_2 are semi-globally bounded.
2. The output of system (1) can track the desired trajectory.
3. The local state constraints are not violated.

Specifically, the tracking errors e_1, e_2 converge automatically to the compact sets $\Omega_{e_1}, \Omega_{e_2}$, respectively, defined by

$$\Omega_{e_1} = \left\{e_1 \in R^n, \|e_{1i}\| \leq \sqrt{b_i^2(1 - e^{-\gamma})}\right\} \quad . . (37)$$

$$\Omega_{e_2} = \left\{e_2 \in R^n, \|e_{2i}\| \leq \sqrt{\frac{\gamma}{\lambda_{\min}(M)}}\right\} \quad . . . (38)$$

Proof: Multiply both sides of equation (34) by $e^{\alpha t}$ yields:

$$\frac{d}{dt}\left(V_2 e^{\alpha t}\right) \leq \lambda e^{\alpha t} \quad . . . . . (39)$$

On both sides of the above formula, while finding the definite integral in the interval $[0,t]$, we obtain

$$V_2 \leq \left(V_2(0) - \frac{\lambda}{\alpha}\right)e^{-\alpha t} + \frac{\lambda}{\alpha} \leq V_2(0) + \frac{\lambda}{\alpha} \quad . . (40)$$

Then, in view of equations (27) and (40), we can derive that $\sum_{i=1}^{n} \ln \frac{b_i^2}{b_i^2 - e_{1i}^2}$ is bounded. Then it is concluded that e_1 and e_2 are bounded.

For $e_1 = q_1 - q_d$ and $||q_d|| \leq Q_d$, we can get that $||q_1|| = ||e_1 + q_d|| \leq ||e_1|| + Q_d$, that is q_1 is bounded. From equation (21), it can be seen that virtual controller β is the function of e_1 and q_d, so β is bounded. With the similar way, we can prove the boundedness of q_2.

From the above analysis, we can see that all signals in the closed-loop system are bounded, and the state constraint is not violated. Based on equation (40), we can get

$$\frac{1}{2}\ln\frac{b_i^2}{b_i^2 - e_{1i}^2} \leq V_2(0) + \frac{\lambda}{\alpha} \quad \|e_{1i}\| \leq \sqrt{b_i^2(1 - e^{-\gamma})} \quad . . . . . (41)$$

where

$$\gamma = 2\left(V_2(0) + \frac{\lambda}{\alpha}\right) \quad . . . . . (42)$$

Similarly for e_2, we obtain

$$\|e_{2i}\| \leq \sqrt{\frac{\gamma}{\lambda_{\min}(M)}} \quad . . . . . (43)$$

Furthermore, by choosing constraint parameters, it can be seen that e_1 can be arbitrarily small. The proof is completed. ■

4. SIMULATION ANALYSIS

In this section, in order to verify the effectiveness of the proposed composite control scheme, a two-DOF robotic manipulator is carried out.

In addition, The disturbance of the system is set as $\tau_d = [0.2\sin t, 0.2\sin t]^T$, the desired trajectory is chosen as $q_d = [sin(2\pi t), sin(2\pi t)]^T$. The output constraint is set as $b = 0.02$, and the control gain K_1,K_2 are set as $diag[60,60]$, respectively.

In this simulation scenario, a nonlinear ESO is performed to estimate disturbance and actuator deviation faults of the manipulator. We set the ESO parameters as follows.

$$\begin{bmatrix} \beta_{01} \\ \beta_{02} \\ \beta_{03} \end{bmatrix} = \begin{bmatrix} 30 \\ 1000 \\ 1500 \end{bmatrix}, \begin{bmatrix} \alpha_1 \\ \alpha_2 \end{bmatrix} = \begin{bmatrix} 0.5 \\ 0.25 \end{bmatrix}, \delta = 0.0025$$

To illustrate the performance of the fault estimation $\hat{\rho}$ compensation composite controller. In this chapter, we present the simulation experiments compared with the sliding mode controller based on model compensation, the controller is as follows

$$\tau = M\ddot{q}_r + C\dot{q}_r + G - K_d s \quad \ldots\ldots\ldots (44)$$

where $K_d = diag(100,100), s = \dot{e} - \Lambda e, \dot{q}_r = \dot{q}_d - \Lambda e$ and $\Lambda = diag(5,5)$. And in the simulation, we assume the parameters of manipulator $M(\dot{q}), C(q,\dot{q}), G(q)$ are known.

Fig 2, 3 show the trajectory tracking performance and velocity tracking performance between the sliding mode control method and the proposed control method respectively. It can be seen from Fig 2 that compared with a sliding mode controller, the proposed control method in this paper can track the actual trajectory effectively, and the error is smaller than that of the sliding mode controller. It can be seen from the local magnification obviously that the sliding mode control has a large error.

Furthermore, fig 4 shows the trajectory errors between different methods respectively. It can be seen from the figure that the error range of proposed method at link 1 is within the range of $[-0.02, 0.02]$, and the error range at link 2 is also within the range of $[-0.01, 0.01]$. The error loss of the control method proposed in this paper always remains within the bounded range of 0.02, and does not violate the predetermined output constraint of $b = 0.02$.

Fig 5 shows the velocity error diagram under different control methods. Similar to trajectory tracking performance, the disturbance compensation control method proposed in this paper also has high performance in velocity tracking. It can be seen from fig 3 that the proposed control method can track the desired trajectory better than the sliding mode control. Furthermore, it can be seen from Fig 5 that the velocity error is relatively small.

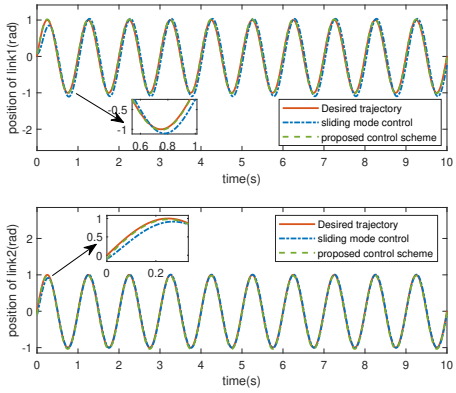


Fig. 2. Tracking performance comparison of different control schemes

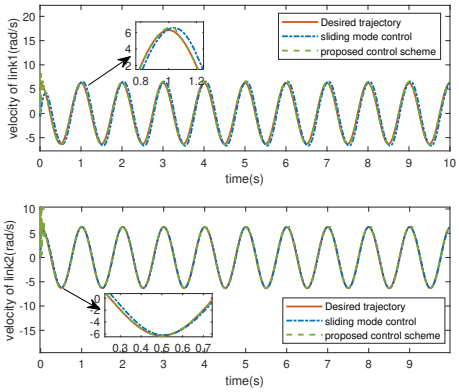


Fig. 3. velocity performance comparison of different control schems

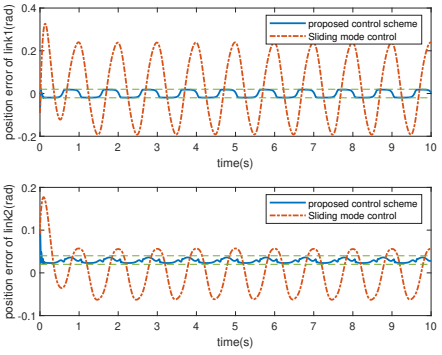


Fig. 4. Tracking errors of the link1 and link2

Fig 6 shows the estimation results of the fault estimate observer, which is used to estimate the multiplicative faults of the actuator. In our paper, the actuator failure ρ is set as $\rho = 0.6$, that is $\tau_{actual} = 0.6\tau$, and the fault estimation observer can estimate the actuator failure value in real time. It can be seen from the figure that the esti-

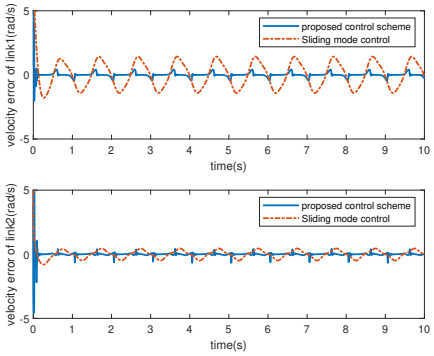


Fig. 5. velocity errors of the link1 and link2

mated value converges rapidly, which ensures the trajectory tracking of the actuator fault trajectory. However, it can also be seen from the above figures that compared with sliding mode control, the speed mutation in the disturbance compensation control scheme is serious, which is related to the desired trajectory. It also indicates that the proposed composite control scheme in this chapter has some disadvantages in tracking a large range of input signals.

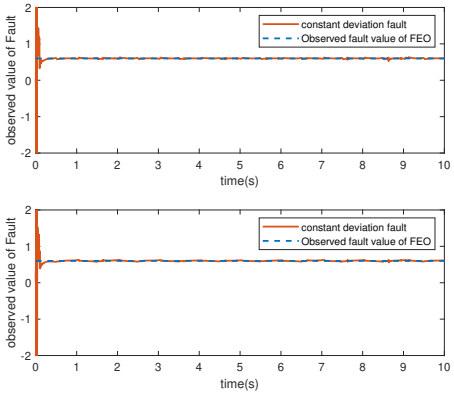


Fig. 6. performance of fault estimation observer

5. Conclusions

For a class of manipulators with external disturbances, output constraints and actuator faults, a composite control scheme was proposed based on fault estimation observer to achieve trajectory tracking. The composite controller used observer to compensate system uncertainty and actuator faults which ensured the stability and robustness of the system. The simulation results have shown that when the robot manipulator exists constant deviation and constant gain faults, the proposed solution has good tracking performance and also keeps the output within bounds.

The method proposed in this paper is suitable for partial failure of the actuators. Further studies need to be performed when the actuators completely fails.

References:

[1] H. Abdi and S. Nahavandi, "Joint velocity redistribution for fault tolerant manipulators", In 2010 IEEE Conference on Robotics, Automation and Mechatronics, pp. 492–497. IEEE, 2010.

[2] Businesswire. "Global Robotic Arm Market Report 2019: Historical Data 2014-2017, 2018 Base Year, 2019 Estimates & Forecasts 2020-2024 - ResearchAndMarkets.com". Website, 2019. https://www.businesswire.com/news/home/20190515005441/en.

[3] F. Caccavale, P. Cilibrizzi, F. Pierri, and L. Villani, "Actuators fault diagnosis for robot manipulators with uncertain model", Control Engineering Practice, 17(1):146–157, 2009.

[4] A. Chakravarty and C. Mahanta, "Actuator fault-tolerant control (FTC) design with post-fault transient improvement for application to aircraft control", International Journal of Robust and Nonlinear Control, 26(10):2049–2074, 2016.

[5] L. Chen, C. Edwards, and H. Alwi, "Integral sliding mode fault tolerant control allocation for a class of affine nonlinear system", International Journal of Robust and Nonlinear Control, 29(3):565–582, 2019.

[6] Z. Chen, Q. Li, X. Ju, and F. Cen, "Barrier Lyapunov function-based sliding mode control for BWB aircraft with mismatched disturbances and output constraints", IEEE Access, 7:175341–175352, 2019.

[7] J. Han, "Active disturbance rejection control technique-the technique for estimating and compensating the uncertainties", National Defense Industry Press, Beijing, pp. 197–270, 2008.

[8] Y. Li and S. Tong, "Adaptive neural networks decentralized FTC design for nonstrict-feedback nonlinear interconnected large-scale systems against actuator faults", IEEE transactions on neural networks and learning systems, 28(11):2541–2554, 2016.

[9] S. Roy, S. B. Roy, and I. N. Kar, "Adaptive–robust control of Euler–Lagrange systems with linearly parametrizable uncertainty bound", IEEE Transactions on Control Systems Technology, 26(5):1842–1850, 2017.

[10] R. R. Selmic and F. L. Lewis, "Deadzone compensation in motion control systems using neural networks", IEEE Transactions on Automatic Control, 45(4):602–613, 2000.

[11] Y. Tanise, K. Taniguchi, S. Yamazaki, M. Kamata, Y. Yamada, and T. Nakamura, "Development of an air duct cleaning robot for housing based on peristaltic crawling motion", In 2017 IEEE International Conference on Advanced Intelligent Mechatronics (AIM), pp. 1267–1272. IEEE, 2017.

[12] K. P. Tee, S. S. Ge, and E. H. Tay, "Barrier Lyapunov functions for the control of output-constrained nonlinear systems", Automatica, 45(4):918–927, 2009.

[13] M. Van, X. P. Do, and M. Mavrovouniotis, "Self-tuning fuzzy PID-nonsingular fast terminal sliding mode control for robust fault tolerant control of robot manipulators", ISA transactions, 96:60–68, 2020.

[14] Y. Wang, B. Li, F. Yan, and B. Chen, "Practical adaptive fractional-order nonsingular terminal sliding mode control for a cable-driven manipulator", International Journal of Robust and Nonlinear Control, 29(5):1396–1417, 2019.

[15] B. Xiao, Q. Hu, and Y. Zhang, "Finite-time attitude tracking of spacecraft with fault-tolerant capability", IEEE Transactions on Control Systems Technology, 23(4):1338–1350, 2014.

[16] L. Zhang, H. Liu, D. Tang, Y. Hou, and Y. Wang, "Adaptive fixed-time fault-tolerant tracking control and its application for robot manipulators", IEEE Transactions on Industrial Electronics, 69(3):2956–2966, 2021.

[17] L. Zhang, Z. Li, and C. Yang, "Adaptive neural network based variable stiffness control of uncertain robotic systems using disturbance observer", IEEE Transactions on industrial electronics, 64(3):2236–2245, 2016.